Surface state mediated plasmon decay in Al(100)

Alessandro Ruocco,[1,*] Wolfgang S. M. Werner,[2] Mario I. Trioni,[3] Stefano Iacobucci,[4] and Giovanni Stefani[1]
[1]*Dipartimento di Scienze Università Roma Tre, Via della Vasca Navale, 84 00146 Roma, Italy*
[2]*Institut fur Angewandte Physik, Vienna University of Technology, Wiedner Hauptstrasse 8-10, A 1040 Vienna, Austria*
[3]*CNR – National Research Council of Italy, ISTM, via Golgi 19, 20133 Milan, Italy*
[4]*CNR – Istituto Struttura della Materia c/o Dipartimento di Scienze Università Roma Tre, Via della Vasca Navale, 84 00146 Roma, Italy*
(Received 17 June 2016; revised manuscript received 23 December 2016; published 6 April 2017)

We present the results of a coincidence experiment aimed at studying the role of plasmons and electronic band structure in the emission of secondary electrons from an Al(100) sample. We measured the spectrum of secondary electrons in coincidence with photoelectrons that have scattered inelastically inside the solid and have excited a bulk plasmon. In this paper we put in evidence that the coincidence energy spectrum of the emitted electron is modulated by the density of occupied states of the sample under investigation. This interpretation is supported by comparing the coincidence energy spectrum with the calculated band structure of the Al(100) surface. The comparison suggests that the coincidence spectrum is dominated by the emission of electrons coming from the Al surface state; it also suggests that, even in the case of bulk plasmon excitation, secondary electron generation is dominated by decay that happens at the immediate surface of the solid.

DOI: 10.1103/PhysRevB.95.155408

I. INTRODUCTION

Plasmons are a general phenomenon characterized by the collective motion of charged particles, occurring in several systems from condensed media [1], to atomic clusters [2], to thin film, and even the ionosphere. More recently, extended macromolecules such as fullerenes have attracted attention for their single molecule collective excitation [3–5]. While the study of plasmon excitation is a well-established argument, much less is known about the decay channels of these collective excitations, even if it is generally accepted that plasmon plays an essential role in the secondary electron (SE) production mechanism [6]. On the other end, the emission of SE is highly relevant for several applications (such as high-energy physics accelerators and storage rings and plasma-wall interaction in a fusion reactor) but gives rise to a featureless spectrum that makes it cumbersome to understand even qualitatively the mechanism of their generation [7]. SE emission is not the only field where plasmon decay plays an important role; for instance, comprehension of the decay mechanism of surface plasmons is of fundamental importance for designing the subwavelength optical components employed in plasmonics and nanophotonics [8].

While the different plasmon excitation channels can be easily discriminated, for instance, with electron energy-loss spectroscopy, the origin of a secondary electron is much more complicated. A possible experiment to gain information on the relationship between plasmon and SE requires the detection of correlated electron pairs, where one electron brings the information on the involved excitation, while the other provides information on decay channels ending with generation of secondary electrons [9–12]. The coincidence technique has been used earlier to establish the causal relationship between energy losses and SE emission [13–15]. Recently, $(e,2e)$ coincidence measurements between electrons that have excited a surface or bulk plasmon (as derived from the energy-loss spectrum) and the secondary electrons provided detailed evidence of the link between excitation of plasmon and emission of electron in the secondary region in solid systems [9,12]. In particular, a recent experiment conducted on single-crystal Be(0001) [12] has shown that secondary electron production undergoes a strong resonant enhancement when the energy lost by the primary electron matches the plasmon frequency. In all these cases the emission of a secondary electron derives from the excitation of a single electron-hole pair following the plasmon decay, and a strong analogy between plasmon decay and photon absorption was established. This implies that plasmons transfer their energy and momentum to an electron of the solid. Subsequently, this electron can be emitted from the solids if the gained energy is large enough to pass the surface barrier potential. If the analogy with photoemission is true and only one electron is involved in the decay of the plasmon, then the band structure of the target must be taken into account for the interpretation of the angular-resolved coincidence spectrum. Previously an $(e,2e)$ experiment on Al(100) [9] put in evidence that part of the emitted electrons in the secondary region are correlated to the decay of surface and bulk plasmon, in particular, a clear edge in the coincidence spectrum was observed at an energy corresponding to the emission from the Fermi level. In the present work, we concentrate the attention on the importance of the band structure, density of states, and binding energy–momentum dispersion of the sample, and in particular of the surface state.

From the theoretical point of view, Kouzakov and Berakdar [16] have calculated the contribution of dielectric screening in the electron-electron collision that gives rise to the emission of secondary electrons in Al and Be; they have found an increase of the cross section at an energy loss corresponding to the plasmon excitation. But in their calculation the electronic structure of the Al and Be was taken into account by a simple jellium model; hence their results cannot be directly compared with our experimental data. Moreover, the dielectric screening

*Corresponding author: alessandro.ruocco@uniroma3.it

effect is not distinguishable, from the experimental point of view, from the excitation and decay of a plasmon because the initial and final state are identical. On the contrary, a recent coincidence experiment on C_{60} [5] with one photon in and two electrons out has been theoretically explained [5] in terms of a three-step model where two of the three steps are the excitation and the decay of a plasmon. In this case the plasmon is not created simultaneously with the photon absorption but by the inelastic scattering of the photoelectron.

In the present work the plasmon decay is studied by measuring the SE spectrum in coincidence with the Al $2p$ photoelectron that lost energy corresponding to the excitation of bulk plasmons. Hence, this is an experiment with one photon in and two electrons out that amounts to a plasmon-mediated double-photoionization experiment. In fact, the process of plasmon excitation associated with the photoemission spectrum is predominantly extrinsic [17,18], i.e., plasmons are created by photoelectrons during their travel inside the sample. Analogously to the experiment on C_{60} [5], we are in presence of a three-step process that can be summarized in the following way: after the photon absorption, the plasmon is excited by the inelastic scattering of the Al $2p$ photoelectron during its travel inside the sample, the plasmon decays, and one electron in the secondary energy region is emitted. In order to distinguish this process from the double photoionization, we call it $(\gamma \rightarrow e,2e)$.

Analysis of the coincidence spectrum confirms that plasmons excited by electron energy losses decay via the emission of one electron in the secondary energy region; the probability of emission in a particular direction and with a given energy is related to the initial density of states of the target. In particular, as a consequence of the chosen experimental kinematics the Al surface state gives a fundamental contribution to the emitted electron in the secondary region after a plasmon decay. In order to support this statement, a detailed knowledge of the surface electronic structure is mandatory. To this end, band structure, including the surface state, and density of states (DOS) of the Al(100) has been calculated in a density functional theory (DFT) framework and the surface energy state has been measured by conventional ultraviolet photoemission spectroscopy (UPS) in the same apparatus and on the same sample used for the coincidence experiment. This result confirms the particular sensitivity of coincidence spectroscopies to the surface of the target, as previously observed and discussed [19,20].

II. EXPERIMENTAL

The measurements have been performed at the Department of Science of the University Roma Tre, with an evolution of the UHV apparatus employed for previous measurements of the plasmon decay [9]. The apparatus is now made of two UHV chambers while the sample is mounted on a manipulator able to travel from the preparation chamber to the analysis chamber. A monochromatic x-ray source from Omicron Gmbh with a photon energy of 148 6.7 eV and a resolution of 320 meV has been added to the previous experimental apparatus. Furthermore, the apparatus includes a He discharge lamp (photon of energy 21.2 and 40.8 eV). The system is provided with two hemispherical analyzers; each analyzer is equipped with a single channel electron multiplier. Pulses from the detectors are processed by two parallel standard electronic chains made by a fast preamplifier, a constant fraction discriminator, a delay line, and a counter directly mounted inside the personal computer (PC) dedicated to data acquisition. In the case of coincidence measurements the output of the two delay lines feeds the input of a time to amplitude converter (TAC) whose output is processed by an analog to digital converter (ADC) directly mounted inside a PC. The time spectra recorded in this way exhibit a peak of true coincidences in the middle of the TAC conversion interval; the position of this peak is controlled by the amount of relative delay inserted before entering the TAC. The typical time resolution of the electronic chain is of the order of 1 ns. The extraction of the true coincidence counts from the time spectrum follows the standard procedure [21]. The Al sample was prepared each day by sputtering (ion energy 4 keV, current on the sample 10 μA), and annealing (450 °C). The intensity of the photon beam was adjusted to equalize the rates of true and false coincidences [21]. Typical true coincidence count rates, which are mainly determined by the acceptance angle of the analyzers (10^{-3} sr), were below 5×10^{-3} Hz under these conditions. The secondary electron spectrum was measured by scanning, in the range 2–15 eV, analyzer 1 (see Fig. 1) in coincidence with the Al $2p$ loss corresponding to the bulk plasmon excitation from the $2p$ photoelectrons ($E_{\mathrm{kin}} = 1393$ eV) measured by analyzer 2.

The geometry of the $(\gamma \rightarrow e,2e)$ experiment is illustrated in Fig. 1. It is to be noted that secondary electrons are collected along directions close to the surface normal. Compared to the previous $(e,2e)$ experiment [9], the scattering geometry is different. In particular, the momentum parallel to the surface of the emitted electron is smaller in the present $(\gamma \rightarrow e,2e)$ experiment. Different scattering geometries give rise to different sampled regions in the energy momentum space, as explained in the following.

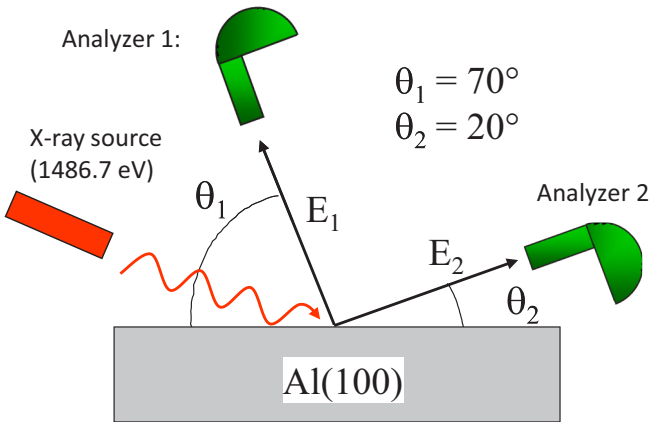

FIG. 1. Geometry of the $(\gamma \rightarrow e,2e)$ experiment. Analyzer 2 is dedicated to collect the Al $2p$ core level and its satellites corresponding to the plasmon excitations, while analyzer 1 is dedicated to scan the energy region of secondary electrons. In the present experiment the secondary electrons are collected close to the normal of the surface.

The energy dispersion of the Al surface state was measured by using the helium discharge lamp with a photon energy of 21.2 eV; photoelectrons were collected with analyzer 1 (see Fig. 1). The source and the analyzer are fixed, the dispersions along the $\overline{\Gamma X}$ and $\overline{\Gamma M}$ directions were obtained by rotating the sample around an axis parallel to the surface, and the surface was azimuthally oriented by means of the low-energy electron diffraction (LEED) technique. The $\overline{\Gamma X}$ orientation was kept fixed in the scattering plane (i.e., the plane containing the scattered and the emitted electrons) in the coincidence experiment.

III. THEORETICAL FRAMEWORK

The *ab initio* electronic structure calculations of the Al(100) surface were carried out in density functional theory [22] within the generalized gradient approximation, employing the Perdew-Burke-Ernzerhof functional [23] to handle exchange and correlation effects. According to the self-consistent method implemented in the SIESTA code [24], the core electrons were described by a separable norm-conserving pseudopotential. The electronic wave function was expanded on a double-ζ polarized numerical orbital basis set. In order to allow a better description of electronic surface states whose wave functions are spatially localized in vacuum, the basis set has been extended in the vacuum region outside the surface layer plane using two layers of Al atomic orbitals. The energy cutoff was fixed to 400 Ry, and the Brillouin zone was sampled by a $12\times12\times1$ Monkhorst-Pack grid [25]. A symmetric slab with 53 Al layers was used for the calculation. The Al atoms of the two outermost layers were relaxed until the residual forces were smaller than 0.01 eV/Å, while the cell size was maintained constant during the calculation fixed by the optimized Al lattice constant ($a = 4.07$ Å).

IV. RESULTS AND DISCUSSION

In Fig. 2 is reported the x-ray photoelectron spectroscopy (XPS) spectrum of the Al $2p$ core level. It is possible to observe the main peak at a kinetic energy of 1408 eV and two loss peaks at about 10 and 15 eV from the main peak corresponding to the excitation of the surface and bulk plasmon, respectively. In the same figure is reported the EELS spectrum taken with a primary energy of 1000 eV (the maximum allowed by the electron gun). The two spectra are very similar, and the differences (background and main peak width) are essentially due to the different kinetic energy and different energy resolution in the two experiments. Plasmons associated with the photoemission process are of two types: intrinsic when the collective excitation is generated in the photon absorption process, extrinsic when plasmons are generated by the photoelectron during its travel inside the matter. Considering the direction of photoemitted electrons (see Fig. 1), only 20% of plasmons are intrinsic [17]. Hence, in this geometry, the majority of the plasmons are extrinsic. These two facts suggest that in the present experiment the photoelectron behaves as an internal electron source of 1408 eV (the energy of $2p$ photoelectrons). In conclusion, this ($\gamma \rightarrow e,2e$) experiment

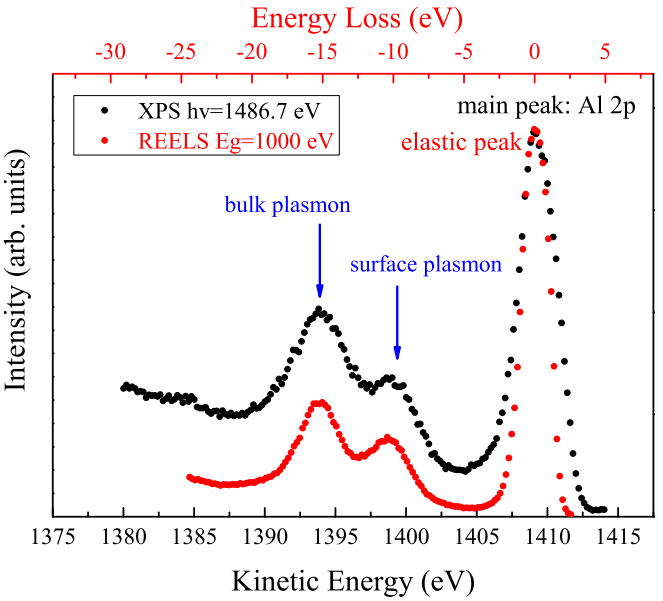

FIG. 2. XPS spectrum of the Al $2p$ core level with its satellites, namely, the bulk and surface plasmon (black dots, lower scale) and energy-loss spectrum taken with a primary energy of 1000 eV (red dots upper scale).

differs from the previous (e,$2e$) study of plasmon decay only concerning the energy of the primary beam and the kinematics of the experiment.

The result of the coincidence experiment is reported in Fig. 3 compared with the secondary noncoincidence spectrum measured with the same analyzer and in the same energy region. The coincidence spectrum was obtained by scanning analyzer 1 in the secondary electron region while analyzer 2 was fixed at 1393 eV, corresponding to the maximum of the XPS Al $2p$ loss originating from the excitation of a bulk plasmon. The conventional secondary spectrum presents

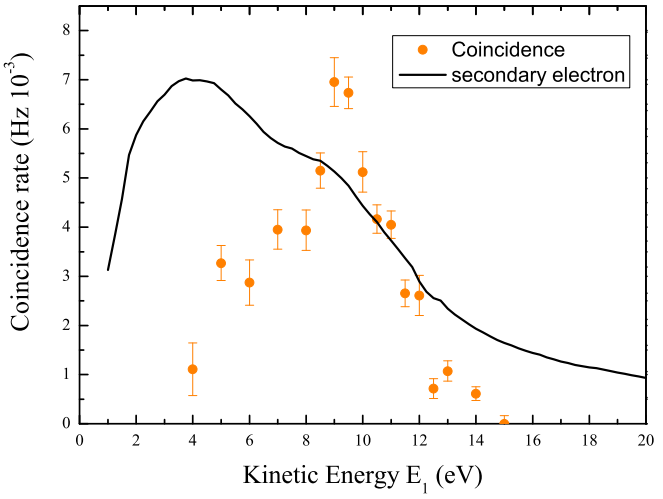

FIG. 3. Secondary spectrum compared to the coincidence spectrum taken with analyzer 2 at fixed energy corresponding to bulk plasmon excitation.

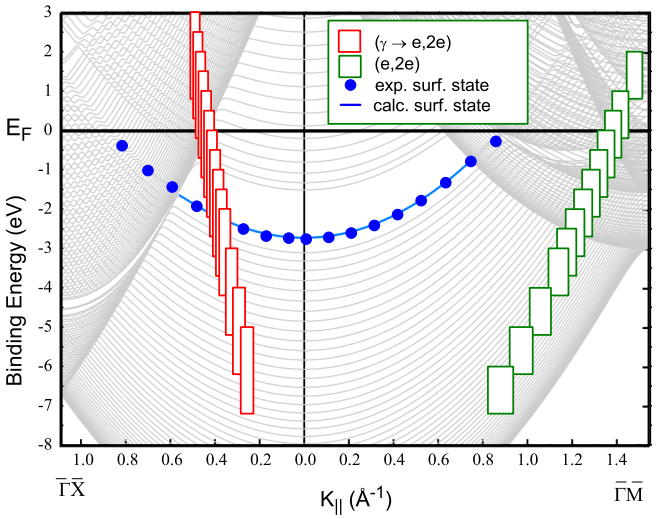

FIG. 4. The energy momentum space of the experiment. The background represents the band structure calculations, the blue dots and continuous line are, respectively, the measured dispersion and the calculated surface state, the red [this ($\gamma \rightarrow e,2e$) experiment] and the green [previous ($e,2e$) coincidence experiment [9]] rectangles are the sampled regions associated with each point of a coincidence spectrum.

a maximum at about 4 eV and a shoulder at about 9 eV. The coincidence spectrum is completely different; it does not show the peak at 4 eV while there is a peak at about 9 eV, and then the signal goes quickly to zero, different from what happens to the conventional secondary spectrum. The only similarity between the spectra is the peak in the coincidence spectrum and the shoulder in the secondary spectrum at 9 eV, the shoulder can be explained as the weak evidence in the conventional secondary spectrum of emitted electrons coming from the bulk plasmons decay. The coincidence spectrum presented here is also different from the previous experiment regarding the decay of bulk plasmon [9], in particular for the presence of the peak at 9 eV. In order to explain the difference between the two coincidence spectra we have to take into account the kinematics of the experimental configuration.

The background of Fig. 4 represents the calculated band structure of the Al(100) surface; the details of the calculations are reported in the theoretical section. The calculated gap has an extension from -3.02 to -1.55 eV at $\bar{\Gamma}$. In the same figure the continuous blue line in the gap represents the calculated Shockley surface state (-2.70 eV at $\bar{\Gamma}$). The measured dispersions of Al surface state along the $\bar{\Gamma}\bar{X}$ and $\bar{\Gamma}\bar{M}$ directions are also reported (blue dots). In this figure the rectangles with the continuous red edge represent the region of the energy momentum space sampled in the present coincidence experiment, while the rectangles with the continuous green edge represent the region sampled in the previous ($e,2e$) experiment [9]. Each rectangle is related to the kinetic energy of the emitted electron, in particular, the energy E_b and the momentum $\mathbf{K}_\parallel$ associated to the center of the rectangle are derived from the conservation laws in the hypothesis that the plasmon decays, transferring its energy and momentum to a single electron of the solid. The two conservation laws are

$$E_b = \hbar\omega_p - E_K - \phi_A, \tag{1}$$

$$\mathbf{K}_\parallel + \mathbf{K}_{\mathbf{p}\parallel} = \mathbf{K}_{\mathbf{e}\parallel}, \tag{2}$$

where E_b, $\hbar\omega_p$, E_K, and ϕ_A are respectively the binding energy of electron in the solid, the energy of the plasmon, the kinetic energy of the emitted electron, and the analyzer work function, and $\mathbf{K}_\parallel$, $\mathbf{K}_{\mathbf{p}\parallel}$, and $\mathbf{K}_{\mathbf{e}\parallel}$ are respectively the momenta, parallel to the surface, of the bound electron inside the sample, of the plasmon, and of the emitted electron. Moreover, the momentum of the plasmon can be related to the energy-loss process that generated the plasmon itself, i.e., $\mathbf{K_p} = \Delta\mathbf{q} = \mathbf{K_f} - \mathbf{K_i}$, where $\mathbf{K_i}$ and $\mathbf{K_f}$ are the momenta of the primary electron and of the scattered electron, respectively. The size of the rectangle is directly related to the experimental energy and momentum acceptances respectively equal to 2.2 eV and 0.045 Å^{-1}. From Fig. 4 we observe that the region sampled by the present experiment intercepts the surface state at a momentum equal to 0.4 Å^{-1}. On the contrary, the momentum of the emitted electron in the case of bulk plasmon decay in the previous ($e,2e$) experiment [9] (rectangles with continuous green edge) does not intersect the Al surface state. The different kinematics and consequently the different sampled regions in the energy momentum space in the two experiments explain the different coincidence spectra obtained in the two cases. In particular, the position of the peak at about 9 eV of kinetic energy can be explained with a direct emission from the surface state, in fact, binding energy and momentum of the peak in the coincidence spectrum correspond to the intersection of the red rectangles presented in Fig. 4 with the measured dispersion of the surface state. In order to support this interpretation, we compare our experimental results with a calculation of the surface DOS, including the surface state, that contains also bulk contributions. The comparison is justified by the fact that all the Al valence states are equivalent in the sense that they originate from the same quasifree electron bands. Consequently, the plasmon decay cross section changes slowly with the energy. The calculations have been computed considering a semi-infinite substrate in the framework of Green's function formalism as implemented in the TRANSIESTA code [26]. The results of the DOS calculations are reported in Fig. 5, together with the experimental coincidence spectrum. The calculated curves are convoluted with a Gaussian whose width is 2.2 eV in order to take into account the experimental resolution.

The different curves have been obtained with a different level of sensitivity to the bulk in order to account for the strong attenuation of the coincidence signal coming from successive layers underneath the surface. The attenuation is modeled by an exponential decay with parametric attenuation length λ. Three of the four curves displayed in Fig. 5 differ for different value of λ ranging from 1 to 5 Å; the fourth curve ($Z = 0$) has been obtained by taking into account only the contribution to the density of states coming from the surface layer. The first observation concerns the agreement between experiment and calculation relative to the peak at 9 eV; the agreement, as expected, does not depend on the particular choice of λ. In the calculated DOS this peak corresponds to the Al surface state, thus confirming the previous statement concerning the

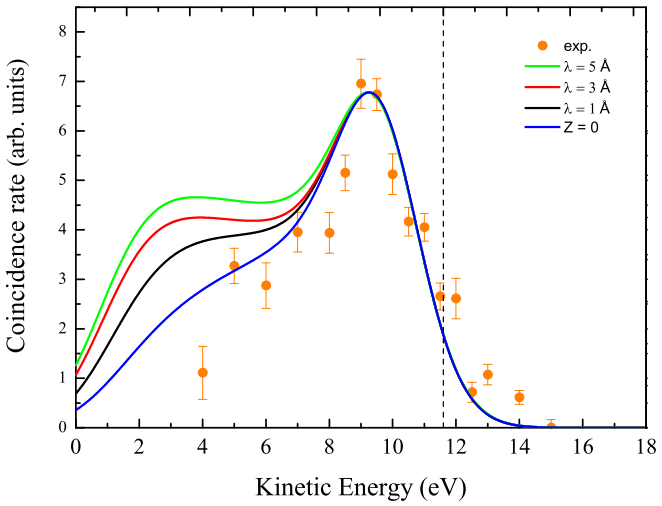

FIG. 5. Coincidence spectrum and DOS calculation as a function of the attenuation length λ. The fourth curve ($z = 0$) is the result of the DOS calculation of the surface layer.

origin of the peak at 9 eV in the coincidence spectrum. The calculated curves differ from each other at lower kinetic energy, where a shoulder becomes more prominent, increasing the bulk contribution. This shoulder is due to the lower part of the DOS. If we limit our integration region to the surface layers, the low-energy part of the DOS is weakened due to the well-known "surface band narrowing," which moves spectral weight from the band edges to the center of the valence band. We observe that the greater the bulk sensitivity, the greater the difference from the experiment, suggesting that the experiment exhibits an extreme surface sensitivity and that in general the proposed model is in agreement with the experiment. The surface sensitivity of the coincidence experiment is peculiar of this technique, as discussed elsewhere [19,20,27], and also when surface states are not involved [28]. Finally, it is noted that also in our earlier work [9] evidence has been found that the emission of secondary electrons as a result of plasmon decay takes place at the immediate surface of the solid. In that work this concerned particularly the decay of the surface plasmon, while the present paper clearly demonstrates that even for the decay of the bulk plasmon the surface plays an important role.

The clear explanation of the coincidence spectrum in terms of density of bulk states and localized surface states suggests that the decay of plasmon gives rise to a process analogous to the photoemission, where the role of the photon is played by the plasmon. In fact, in this single-particle picture the energy and the momentum of the plasmon is transferred to a single bound electron that is emitted from the solid into the vacuum. In this model, the maximum allowed kinetic energy of the emitted electron is given by $E_K^{\max} = \hbar\omega_p - \phi_A$, corresponding to the emission of an electron coming from the Fermi level of Al, as clearly pointed out in our previous work [9]. In the present work the Fermi level is not clearly detectable because the spectrum is dominated by the surface state. The position of the surface state in the coincidence spectrum can be derived from the energy conservation law in Eq. (1), where E_b is, in this case, the binding energy of the surface state, thus confirming that only one electron of the solid is involved in the decay process of the plasma oscillation. The inelastic scattering cross section at this energy is essentially in forward direction, analogous to what happens in specular reflection [29]; then the plasmons selected in the coincidence experiment have small momentum (0.1 Å^{-1}) compared with the critical wave vector ($K_c = 1.3$ Å^{-1} in Al [30]), where the dispersion curve of the bulk plasmon intersects the single electron excitation band. It is well known that plasmon with a momentum greater than K_c has a very short lifetime due to its superposition with intraband excitation, while below K_c lifetime is longer because intraband transitions are forbidden and electrons involved in the decay of plasmons make a near vertical interband transition. Bocan and Miraglia [31,32], in their semiclassical approach to the problem of plasmon decay, considered alternatively to the interband near vertical transition also a second channel where two interacting electrons share the energy and the momentum of the plasmon. This second channel does not seem to be relevant in our experiments because it should give rise to a continuous energy sharing between the two final electrons. On the contrary, we observe a distribution due to a single particle density of states, such as the peak from the surface state or from the Fermi level. The kinematics condition of this experiment determines the predominance of the interband transition channel with respect to the two interacting electrons channel [32]. An alternative channel that gives rise to an intraband transition involves a phonon plus an electron in place of two interacting electrons in order to satisfy the momentum conservation; this channel should represent a minor contribution to the decay of plasmon, as pointed out in another calculation [33].

V. CONCLUSIONS

Our ($\gamma \rightarrow e,2e$) coincidence spectrum is compatible with the three-step model [5] in which an extrinsic plasmon is created and decays, transferring its energy and momentum to a single bound electron that is consequently emitted into the vacuum contributing to the coincidence spectrum in the secondary electron energy region. In this model the conservation of the parallel momentum must be considered. Then, as evident from Eq. (2), the band structure of the target plays a fundamental role. This is confirmed by the comparison of the experimental data with the density of states calculation, where in particular, the peak in the coincidence spectrum is attributed to the emission of an electron from the Al surface state. On the other hand, calculations that take into account both the dynamics of the interaction and the real band structure are not available at the moment. Thus, further theoretical calculations based on the direct scattering model [16], including the real surface band structure, are desirable in order to shed more light on the role of the plasmon in the ($e,2e$) collision at metallic surfaces. The relevance of the band structure, and in particular of the surface state in the decay of bulk and surface plasmons, has been put in evidence also in a recent ($e,2e$) experiment on Be(0001) [12]. This suggests that the coupling of the collective excitation with the band structure of the solids is a more general phenomenon, independent from the details of the excitation and from the sample investigated, at least in this class of nearly free electron metals. Unlike all previous investigations of the plasmon decay mechanism [9–12], due to the high photon energy, exchange and correlation between photoelectron and ejected electron can be

disregarded and the observed correlation between plasmon excitation and secondary electron generation is a clear evidence for long-range (plasmon)–short-range (electron-hole) coupling.

ACKNOWLEDGMENT

Partial financial support by the FP7 People: Marie-Curie Actions Initial Training Network (ITN) SIMDALEE2 (Grant No. PITN 606988) is greatly acknowledged.

[1] D. Pines and D. Bohm, Phys. Rev. **85**, 338 (1952).
[2] W. A. de Heer, Rev. Mod. Phys. **65**, 611 (1993).
[3] A. V. Verkhovtsev, A. V. Korol, A. V. Solovyov, P. Bolognesi, A. Ruocco, and L. Avaldi, J. Phys. B: At., Mol. Opt. Phys. **45**, 141002 (2012).
[4] P. Bolognesi, L. Avaldi, A. Ruocco, A. Verkhovtsev, A. V. Korol, and A. V. Solovyov, Eur. Phys. J. D **66**, 254 (2012).
[5] M. Schler, Y. Pavlyukh, P. Bolognesi, L. Avaldi, and J. Berakdar, Sci. Rep. **6**, 24396 (2016).
[6] M. S. Chung and T. E. Everhart, Phys. Rev. B **15**, 4699 (1977).
[7] Y. Lin and D. C. Joy, Surf. Interface Anal. **37**, 895 (2005).
[8] J. M. Pitarke, V. M. Silkin, E. V. Chulkov, and P. M. Echenique, Rep. Prog. Phys. **70**, 1 (2007).
[9] W. S. M. Werner, A. Ruocco, F. Offi, S. Iacobucci, W. Smekal, H. Winter, and G. Stefani, Phys. Rev. B **78**, 233403 (2008).
[10] W. S. M. Werner, F. Salvat-Pujol, A. Bellissimo, R. Khalid, W. Smekal, M. Novák, A. Ruocco, and G. Stefani, Phys. Rev. B **88**, 201407 (2013).
[11] S. Samarin, J. Berakdar, A. Suvorova, O. M. Artamonov, D. K. Waterhouse, J. Kirschner, and J. F. Williams, Surf. Sci. **548**, 187 (2004).
[12] G. Di Filippo, D. Sbaraglia, A. Ruocco, and G. Stefani, Phys. Rev. B **94**, 155422 (2016).
[13] D. Voreades, Surf. Sci. **60**, 325 (1976).
[14] F. J. Pijper, Ph.D. dissertation, Technische Universiteit Delft, 1993.
[15] H. Mullejans, A. L. Bleloch, A. Howie, and M. Tomita, Ultramicroscopy **52**, 360 (1993).
[16] K. A. Kouzakov and J. Berakdar, Phys. Rev. A **85**, 022901 (2012).
[17] F. Yubero and S. Tougaard, Phys. Rev. B **71**, 045414 (2005).
[18] W. J. Pardee, G. D. Mahan, D. E. Eastman, R. A. Pollak, L. Ley, F. R. McFeely, S. P. Kowalczyk, and D. A. Shirley, Phys. Rev. B **11**, 3614 (1975).
[19] A. Liscio, R. Gotter, A. Ruocco, S. Iacobucci, A. G. Danese, R. A. Bartynski, and G. Stefani, J. Electron Spectrosc. Relat. Phenom. **137–140**, 505 (2004).
[20] W. S. M. Werner, W. Smekal, H. Störi, H. Winter, G. Stefani, A. Ruocco, F. Offi, R. Gotter, A. Morgante, and F. Tommasini, Phys. Rev. Lett. **94**, 038302 (2005).
[21] G. Stefani, L. Avaldi, and R. Camilloni, in *New Directions in Research with Third-Generation Soft X-Ray Synchrotron Radiation Sources*, edited by A. S. Schlachter and F. J. Wuilleumier, NATO ASI Series Vol. 254 (Springer, Netherlands, 1994), p. 161.
[22] P. Hohenberg and W. Kohn, Phys. Rev. **136**, B864 (1964).
[23] J. P. Perdew, K. Burke, and M. Ernzerhof, Phys. Rev. Lett. **77**, 3865 (1996).
[24] J. M. Soler, E. Artacho, J. D. Gale, A. García, J. Junquera, P. Ordejón, and D. Sánchez-Portal, J. Phys.: Condens. Matter **14**, 2745 (2002).
[25] H. J. Monkhorst and J. D. Pack, Phys. Rev. B **13**, 5188 (1976).
[26] M. Brandbyge, J.-L. Mozos, P. Ordejón, J. Taylor, and K. Stokbro, Phys. Rev. B **65**, 165401 (2002).
[27] F. O. Schumann, C. Winkler, and J. Kirschner, Phys. Rev. B **88**, 085129 (2013).
[28] W. S. M. Werner, F. Salvat-Pujol, W. Smekal, R. Khalid, F. Aumayr, H. Störi, A. Ruocco, and G. Stefani, Appl. Phys. Lett. **99**, 184102 (2011).
[29] A. Ruocco, M. Milani, S. Nannarone, and G. Stefani, Phys. Rev. B **59**, 13359 (1999).
[30] H. Raether, *Excitation of Plasmons and Interband Transitions by Electrons* (Springer, Berlin, 1980).
[31] G. A. Bocan and J. E. Miraglia, Phys. Rev. A **69**, 012901 (2004).
[32] G. A. Bocan and J. E. Miraglia, Phys. Rev. A **71**, 024901 (2005).
[33] K. Sturm and L. E. Oliveira, Phys. Rev. B **24**, 3054 (1981).